Progress In Electromagnetics Research M, Vol. 35, 183–191, 2014

Information Content Analysis for the Millimeter and Sub-Millimeter Wave Atmospheric Sounding Data from Geostationary Orbit

Hai-Bo Zhao*, Cheng Zheng, Yong-Fang Zhang, Bin Liang, Nai-Ming Ou, and Jun-Gang Miao

Abstract—Operating frequencies for passive remote sensing have been extended to millimeter and sub-millimeter wave regions in recent years. Due to relatively shorter wavelengths, narrower beam widths can be achieved under antenna size limitations. In turn, better spatial resolution can be achieved, which is especially important for sensors in geostationary orbit. There are several mission proposals for millimeter and sub-millimeter wave payloads in geostationary orbit, e.g., Geostationary Observatory for Microwave Atmospheric Sounding (GOMAS) proposed by European countries, Geosynchronous Microwave (GEM) Sounder/Imager Observation System proposed by USA, the next generation Chinese geostationary orbit meteorological satellite FY-4, etc. The feasibility study of geostationary microwave payloads and simulation of millimeter and sub-millimeter wave atmospheric sounding data is currently underway. Many measures evaluate the efficacy of atmospheric sounding data, one of which is the Degrees of Freedom for Signal (DFS). It is independent of specific regression algorithm thus able to offer an objective measure for performance comparison and channel parameter optimization. In this paper, the DFS of a set of millimeter wave ($50 \sim 70$ GHz, 118 GHz, 183 GHz) and sub-millimeter wave (380 GHz, 425 GHz) sounding channels is analyzed. The DFS improvement with increasing bandwidth is given; results suggest that broader channel bandwidth will improve the efficacy and retrieval performance of the future geostationary orbit millimeter and sub-millimeter wave radiometers.

1. INTRODUCTION

Geostationary orbit (GEO) has its unique advantages over low earth orbit (LEO) in meteorological applications [1–3]. At a height of 36000 km, a satellite instrument is able to observe a wide area across $\pm 70^\circ$ latitude and longitude and to continuously monitor a designated area with typical temporal resolution of $0.5 \sim 1$ hour. To fulfill special requests, it is able to complete a scan of a small area within $3 \sim 5$ minutes. Due to its high temporal resolution, geostationary satellites are desirable to continuously monitor the development of cloud systems and of short lifecycle mesoscale systems leading to rainstorm, snowstorm, hailstorm, typhoon, etc. However, since the height of GEO is $40 \sim 50$ times higher than that of LEO, the spatial resolution would be $40 \sim 50$ times poorer assuming the same operating frequency and antenna size.

There are two fundamental ways to improve spatial resolution of a microwave radiometer: (1) increasing the antenna size, (2) increasing the operating frequency. For GEO application, to achieve 50 km spatial resolution for the millimeter wave (e.g., $50 \sim 70$ GHz) radiometer will require the antenna diameter to be $4 \sim 5$ m. Such large antenna size will pose a tremendous difficulty for the launch vehicle with current technology.

On the other hand, there is the approach to increase the operating frequency of the radiometer, thus in turn to achieve narrower beam width and higher spatial resolution with traditional real aperture antenna. There are several oxygen and water vapor absorption bands available for atmospheric sounding

Received 19 February 2014, Accepted 1 April 2014, Scheduled 9 April 2014

* Corresponding author: Hai-Bo Zhao (zhaohaibo0813@126.com).

The authors are with the Electromagnetics Engineering Laboratory, Beihang University, Beijing 100191, China.

in the microwave, millimeter-wave and sub-millimeter wave spectrum: for temperature sounding there are 50–70 GHz, 118 GHz, 425 GHz, etc., and for water vapor sounding there are 22 GHz, 183 GHz, 325 GHz, 380 GHz, etc. Currently the most commonly used sounding bands by space-borne radiometers are 50–70 GHz and 183 GHz. Those radiometers include: SSM/IS, AMSU, MHS, HSB, ATMS, etc. In recent years, the possibility of millimeter and sub-millimeter wave sounding on the geostationary orbit has been studied, and several such conceptual radiometers have been proposed.

In 1998, NASA and NOAA jointly proposed the Geosynchronous Microwave (GEM) Sounder/Imager Observation System which includes sounding bands: 50–70 GHz, 118 GHz, 183 GHz, 380 GHz, and 425 GHz [4]. In 2002 several European and USA agencies proposed Geostationary Observatory for Microwave Atmospheric Sounding (GOMAS) [5], which has identical sounding bands. By using sub-millimeter wave frequencies and affordable antenna size (~ 3 m), the spatial resolution can be improved to ~ 30 km (see Table 1 of Section 2.1), and this performance satisfies the requirements for nowcast given by EUMETSAT [1–6].

Millimeter and sub-millimeter wave sounding in geostationary orbit has attracted much attention in recent years. This paper will examine the performance of those sounding channels. The baseline channel characteristics (sounding bands, center frequencies) are those proposed by GOMAS, GEM and FY-4. Through simulation, the authors find that by increasing the bandwidth of sounding channels the efficacy (in term of DFS) has increased, and the sounding performance (in term of accuracy) has improved.

2. METHODOLOGY

2.1. Selection of Baseline Channels

The initial baseline bandwidth and center frequency proposed by GEM, GOMAS and FY-4 are plotted in Figures 1–5. Light blue bands represent the original bandwidth, and dark blue represents 80% maximum bandwidth (detailed in description can be found in Section 2.5). The expected nadir horizontal resolutions are listed in Table 1.

There are total of 5 sounding bands, in which 50 GHz, 118 GHz, 425 GHz are for temperature sounding and 183 GHz, 380 GHz for water vapor sounding. 50 GHz and 183 GHz are heritage sounding bands. Although they may not satisfy the horizontal resolution requirement, they are included for risk reduction considerations. The new sub-millimeter bands 380 GHz and 425 GHz are required to achieve ~ 10 km horizontal resolution. However, because of strong oxygen and water vapor absorption, it is difficult for the sub-millimeter sounding bands to retrieve near surface atmospheric information (as can be seen in Section 2.3, channel weighting functions approach zero near surface). Therefore, again the complementary 50 GHz and 183 GHz sounding bands are necessary. 118 GHz sounding band provides moderate resolution (~ 40 km) and better channel sensitivity than 425 GHz band; therefore it is also considered in this paper.

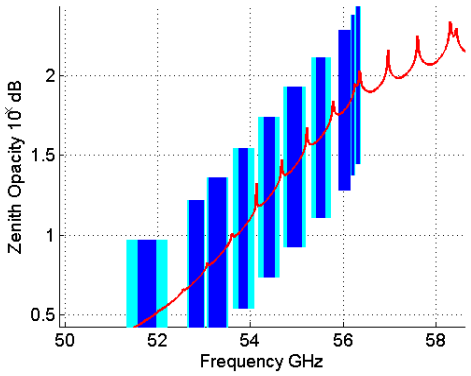

Figure 1. Channel bandwidth for 50 GHz sounding band (Dark bands: original bandwidth, light bands: 80% of maximum bandwidth, same color coding is used throughout Figures 2–5).

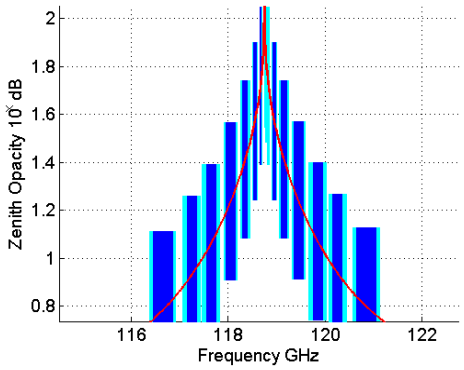

Figure 2. Channel bandwidth for 118 GHz sounding band.

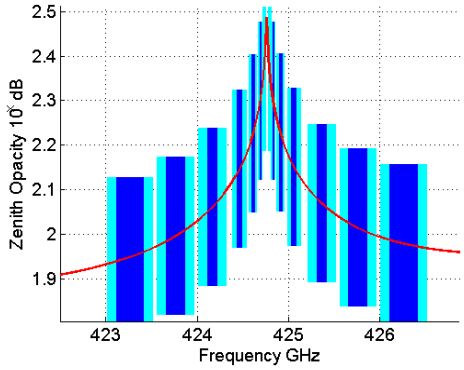

Figure 3. Channel bandwidth for 425 GHz sounding band.

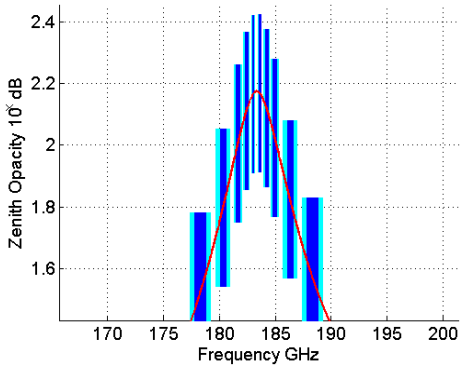

Figure 4. Channel bandwidth for 183 GHz sounding band.

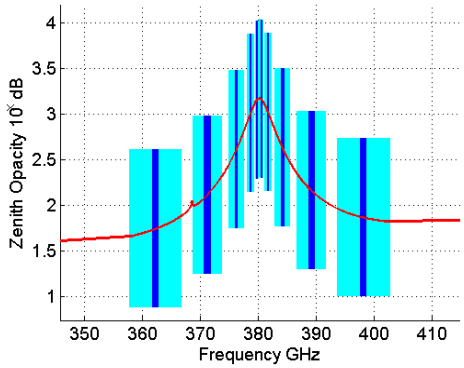

Figure 5. Channel bandwidth for 380 GHz sounding band.

Table 1. Nadir horizontal resolution from geostationary orbit with respect to antenna diameter and operating frequency [13].

Antenna Diameter	50 GHz	118 GHz	183 GHz	380 GHz	425 GHz
1 m	242 km	112 km	73 km	35 km	31 km
2 m	121 km	56 km	36 km	18 km	16 km
3 m	81 km	37 km	24 km	12 km	10 km
4 m	60 km	28 km	18 km	8.8 km	7.8 km

2.2. Selection of Atmospheric Profiles

The atmospheric profiles used in this study are Seebor V5.0 training dataset, which includes 15704 all-season globally distributed atmospheric profiles from variety of sources, such as NOAA-88, TIGR-3, radiosonde, and ECMWF. Each profile contains temperature, humidity and ozone information at 101 pressure levels. Mean value, standard deviation and covariance matrices for temperature and water vapor are shown in Figures 6–7.

2.3. Weighting Function for Proposed Channels

The weighting function is essential in analyzing sensor efficacy (detailed in Section 2.4), and the weighting functions of baseline sounding channels are shown in Figures 8–12.

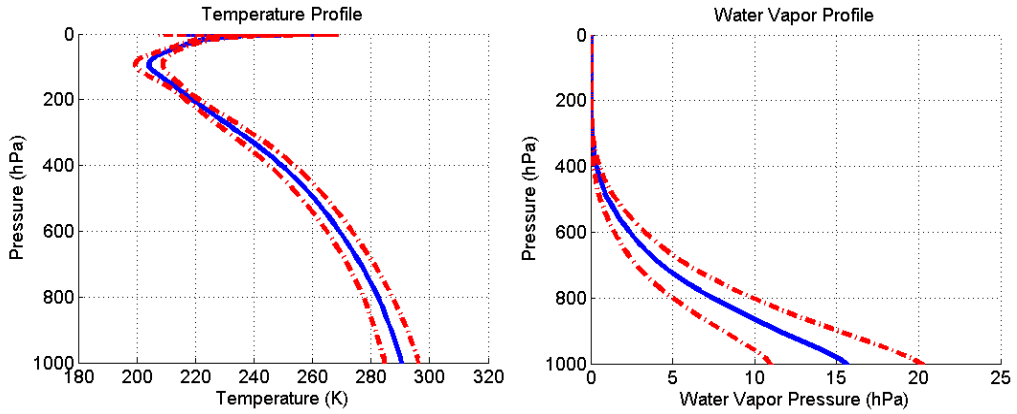

Figure 6. Mean and standard deviation for temperature and water vapor profiles.

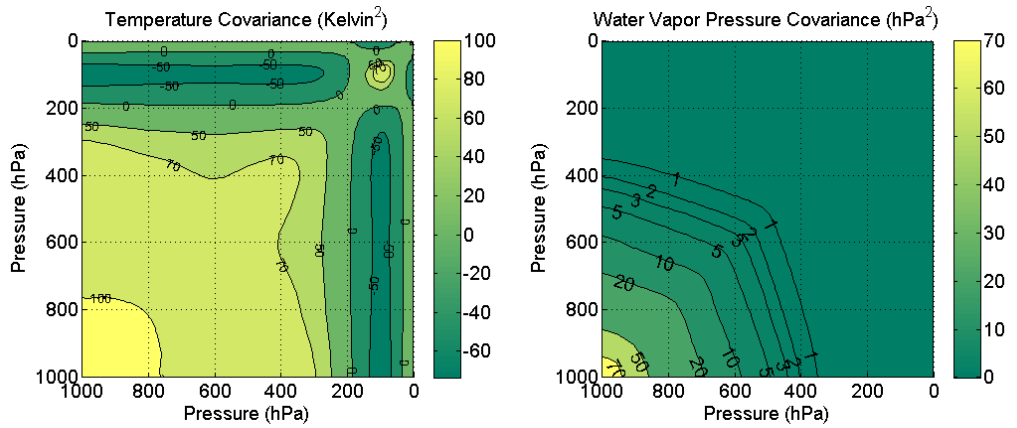

Figure 7. Temperature and water vapor covariance matrices.

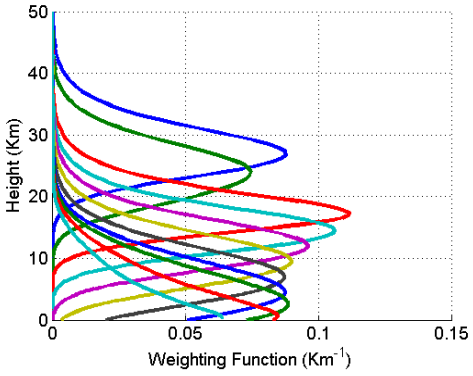

Figure 8. Channel weighting functions for 50 GHz sounding band.

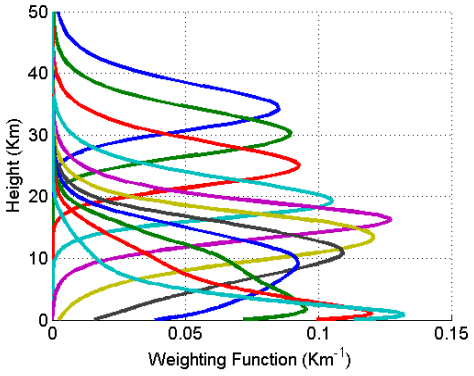

Figure 9. Channel weighting functions for 118 GHz sounding band.

2.4. DFS of Sounding Channel Bands

The DFS has been utilized to study the efficacy of atmospheric remote sensing data by many authors [6–12]. For consistency and clarity it is reiterated in this section.

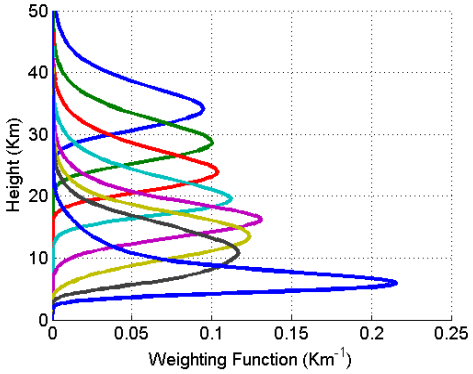

Figure 10. Channel weighting functions for 425 GHz sounding band.

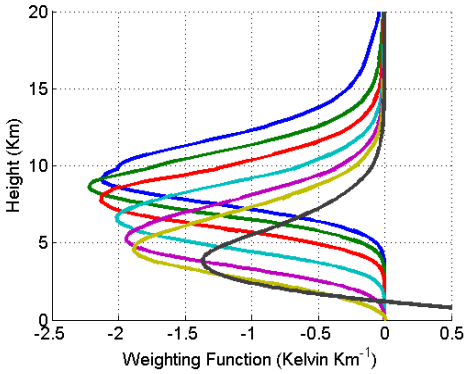

Figure 11. Channel weighting functions for 183 GHz sounding band.

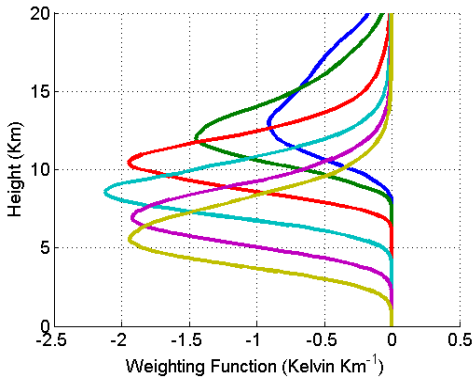

Figure 12. Channel weighting functions for 380 GHz sounding band.

If a Gaussian probability distribution is assumed for an atmospheric vector x, the covariance matrix of atmospheric state after measurement can be expressed as:

$$\mathbf{A}^{-1} = \mathbf{B}^{-1} + \mathbf{K}^T\mathbf{E}^{-1}\mathbf{K} \tag{1}$$

where $\mathbf{B}$ is the covariance matrix of atmospheric state before measurement; $\mathbf{E}$ is the covariance matrix of sensor noise.

In practice, matrix $\mathbf{B}$ has significant off-diagonal elements implying strong correlations between atmospheric states at different altitudes. A transformation can be conducted as follows so as to reduce $\mathbf{B}$ and $\mathbf{E}$ to a unit matrix:

$$\begin{aligned}
\tilde{x} &= \mathbf{B}^{-1/2}x \\
\tilde{y} &= \mathbf{A}^{-1/2}y \\
\tilde{\mathbf{B}} &= \mathbf{B}^{-1/2}\mathbf{B}\mathbf{B}^{-1/2} = \mathbf{I} \\
\tilde{\mathbf{E}} &= \mathbf{E}^{-1/2}\mathbf{E}\mathbf{E}^{-1/2} = \mathbf{I} \\
\tilde{\mathbf{K}} &= \mathbf{E}^{-1/2}\mathbf{K}\mathbf{B}^{1/2} \\
\tilde{\mathbf{A}}^{-1} &= \tilde{\mathbf{K}}^T\tilde{\mathbf{E}}^{-1}\tilde{\mathbf{K}} + \tilde{\mathbf{B}}^{-1}
\end{aligned} \tag{2}$$

where I is identity matrix. This process is called by Rodgers as prewhitening, as it transforms noise into white noise. Matrix power is calculated in the following fashion:

$$\mathbf{B}^{-1/2} = \left(\mathbf{L}\mathbf{\Lambda}\mathbf{L}^T\right)^{-1/2} = \mathbf{L}\mathbf{\Lambda}^{-1/2}\mathbf{L}^T \tag{3}$$

The diagonal matrix $\mathbf{\Lambda}$ is composed of the eigenvalues of $\mathbf{B}$, and $\mathbf{L}$ is composed of the respective eigenvectors of $\mathbf{B}$.

To this end, a parameter called DFS can be defined as:

$$\mathrm{DFS} = d_s = \mathrm{trace}(\mathbf{D_s}) = \mathrm{trace}\left(\mathbf{I} - \tilde{\mathbf{A}}\right) \tag{4}$$

DFS has many desirable properties: (1) It is always less than or equal to (precise measurements) the number of independent measurements. (2) It gives correct asymptotic behavior when the measurement noise is approaching infinite. (3) It favors even distribution of information density, whereas Shannon entropy reduction favors high measurement precision. DFS is a scalar and global measure that quantifies the effectiveness of sounding data, while the diagonal of $\mathbf{D}_s$ is able to represent DFS density at different altitudes. The DFS density of respective sounding channels is shown in Figure 13; the expected channel sensitivity is adopted from literature [14].

It can be seen from Figure 9 that 118 GHz sounding band has the best performance at high altitude ($25 \sim 50$ km). Although the 425 GHz band in Figure 10 has similar high altitude sounding channels, their performance is relatively poor due to large channel noise. The mid-altitude sounding performances for 50 GHz, 118 GHz and 425 GHz are comparable. Since atmospheric absorption for 425 GHz is high, and the lower atmosphere appears opaque, the low-altitude and near-surface sounding performance for 425 GHz band is significantly inferior to that of 50 GHz and 118 GHz bands. It should be noted that 425 GHz band alone cannot perform all-altitude temperature sounding; additional sounding channels at 50 GHz and 118 GHz must be accompanied.

As for water vapor sounding, 183 GHz has superior performance at low altitudes ($0 \sim 6$ km), and 380 GHz has superior performance at high altitudes ($8 \sim 12$ km). For the same reason as the 425 GHz band, the 380 GHz alone cannot perform all-altitude water vapor sounding either.

2.5. DFS vs. Bandwidth

On close observation of the GOMAS channel parameters, we can notice that the sensitivity for the channels near absorption peak does not satisfy the required sensitivity, and this problem is especially prominent for sub-millimeter wave sounding bands. For radiometers, the channel sensitivity (Snt) is approximately proportional to equivalent system noise temperature T_{sys}, which is dependent on hardware performance and is inversely proportional to the square root of the product of bandwidth (B) and observing time (τ).

$$Snt \approx \frac{T_{sys}}{\sqrt{B\tau}} \tag{5}$$

In order to improve channel sensitivity, one can consider reducing T_{sys} and increasing τ, B. Unfortunately, T_{sys}, and τ are constrained by hardware and scanning requirements; therefore it is more practical to increase the bandwidth in order to achieve better channel sensitivity.

Apparently, the possible maximum bandwidth for each sounding channel is achieved when the passbands are conterminous to each other, but this is not possible in practice since there is no filter with ideal rectangular roll-off and since real filters have signal spill-over between adjacent channels. Therefore, we examine the performance when the actual bandwidth approaches 80% of the maximum bandwidth. The original bandwidth is shown in Figures 1–5 as dark bands, and 80% of the maximum bandwidth is shown as light bands.

By gradually increasing bandwidth, the expected channel sensitivity is improved accordingly. The DFS vs. bandwidth increase is shown in Figure 14.

DFS corresponding to different sounding bands exhibits different amounts of improvement: for 50 GHz there is a 0.5 increase; for 118 GHz there is a 0.25 increase; for 425 GHz there is a 0.9 increase; for 183 GHz there is a 0.5 increase; for 380 GHz, there is a 0.6 increase. As can be expected, the sub-millimeter wave sounding bands show the most prominent improvement, because of their high level of noise. By increasing the channel bandwidth, this problem is ameliorated.

2.6. Retrieval Performance

With Seebor V5.0 training dataset, the retrieval performance was simulated, as shown in Figures 15–16. It should be noted that simulated retrieval error is larger than that of the operational performance,

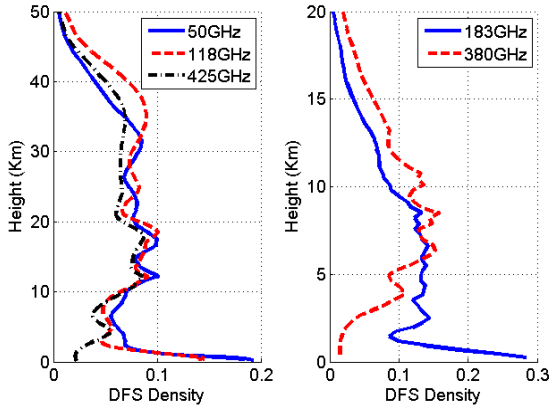

Figure 13. DFS density over altitude, temperature sounding channels are shown in the left, water vapor sounding channels are shown in the right.

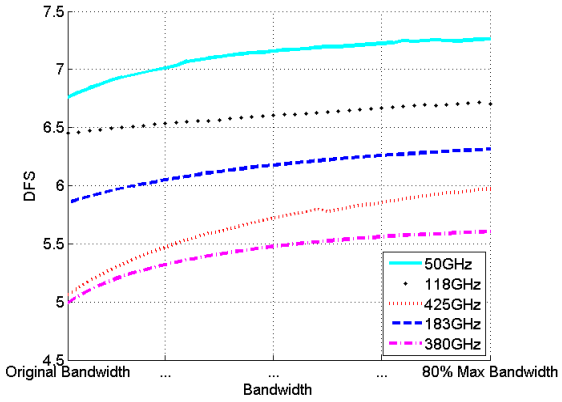

Figure 14. DFS with respect to bandwidth.

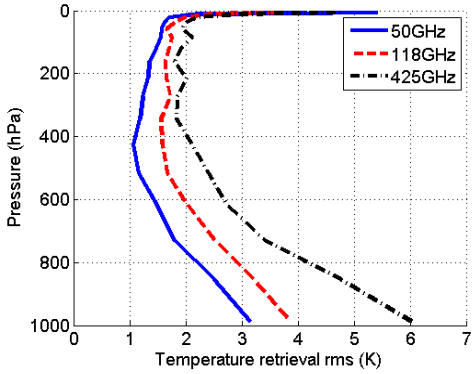

Figure 15. Temperature retrieval performance.

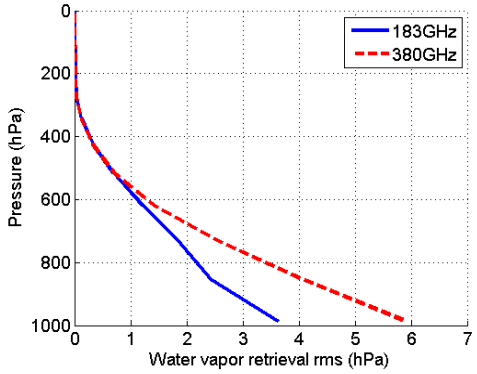

Figure 16. Water vapor retrieval performance.

due to global selection of training profiles, i.e., the training dataset has large rms, and *a-priori* information concerning climate, season and possible weather condition is varied. Therefore, this retrieval performance can be considered as worst-case scenario.

The artificial neural network used in this study consists of one hidden layer of 10 log-sig neurons. The Levenberg-Marquardt back-propagation algorithm is used to train the network.

It can be seen from the following figures, 50 GHz sounding band has the best sounding performance. The 118 GHz, 425 GHz sounding bands have the worst performance, especially in the lower troposphere because of water vapor absorption and variation.

For water vapor sounding, 183 GHz is superior to 380 GHz since the former has a great number of channels and higher channel sensitivity. The strong absorption of water vapor around 380 GHz directly causes that the neural network cannot effectively retrieve near-surface water vapor information.

Now we will examine the performance of sounding channels with 80% of the maximum bandwidth and adjust channel sensitivity according to (5). An identical neural network configuration is used; the temperature and water vapor retrieval improvement over the original configuration are shown in Figures 17–18. For temperature retrieval, the sub-millimeter wave sounding band 425 GHz has a more prominent improvement followed by 118 GHz and 50 GHz, which is consistent with the analysis in Section 2.5. For water vapor retrieval, 380 GHz shows greater improvement than 183 GHz band.

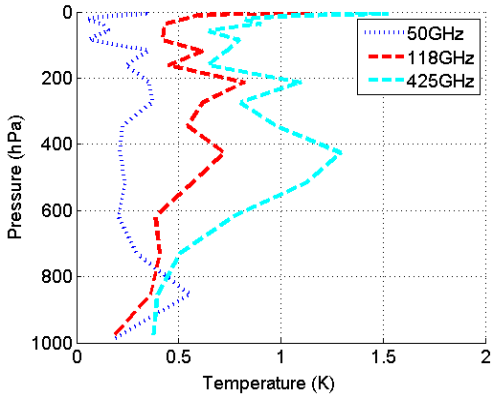

Figure 17. Temperature retrieval performance improvement.

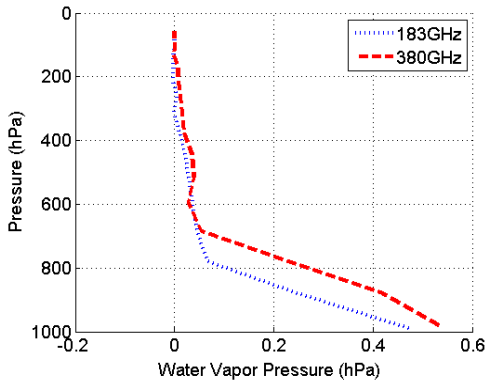

Figure 18. Water vapor retrieval performance improvement.

3. CONCLUSION AND FUTURE WORK

In this paper, the information content of the sounding data for the future GOMAS-like geostationary sounder is analyzed by an objective measure, i.e., DFS, the performance for different sounding bands is examined, and the improvement of sounding performance with increased channel bandwidth is presented.

It can be concluded that though the sub-millimeter wave sounding bands will offer the required horizontal resolution with affordable antenna size, the temperature and water vapor sounding performance is inferior to that of the traditional millimeter-wave bands. Therefore, even though traditional sounding bands, i.e., 50 GHz, 183 GHz, do not meet the horizontal resolution requirements under current antenna size limitation in geostationary application, they are still irreplaceable.

Noticeable performance improvements can be realized by increasing passband of sounding channels. Wider passband will smooth out vertical sounding details, but will also improve channel sensitivity. This is a typical optimization problem with constraint of maximum bandwidth, and by simulation it can be seen that with 80% maximum bandwidth the DFS and retrieval performance have been improved. Therefore, it is recommended that with acknowledging hardware limitations bandwidth of sounding channels is increased.

The future work following this study may include: (1) Refining the selection of training profile, and dividing them into smaller groups according to different season and climatology. In this way, more *a-priori* knowledge is included, so the trained neural network will have better retrieval performance. (2) The information measure DFS is suited for optimization of channel parameters, which includes the number of channels, center frequencies and bandwidths of channels, etc. But in this way, the optimization will discard the framework of the initial baseline of GOMAS, thus it is beyond the scope our current paper. (3) Furthermore, the addition of complementary infrared sounding data to sub-millimeter wave sounding data is another interesting and practical objective, which will be addressed in the future with the application of sub-millimeter wave radiometer on geostationary orbit.

ACKNOWLEDGMENT

The authors wish to acknowledge the financial support from the Electromagnetics Laboratory of Beihang University and the valuable advice from the Microwave Remote Sensing Group.

REFERENCES

1. WMO report SAT-21, "Statement of guidance regarding how well satellite capabilities meet WMO user requirements in several application areas," WMO TD No. 992, Geneva, Switzerland, 2000.

2. Lambrigtsen, B. H., S. T. Brown, S. J. Dinardo, P. P. Kangaslahti, A. B. Tanner, and W. J.Wilson, "Progress in developing GeoSTAR — A microwave sounder for GOES-R," *Proceedings of SPIE*, 1–9, Aug. 2005.
3. Carlstrom, A., J. Christensen, J. Embretsen, A. Emerich, and P. Maagt, "A geostationary atmospheric sounder for now-casting and short-range weather forecasting," *Proceedings of SPIE,* Vol. 5882, 1–4, Jun. 2009.
4. Gasiewski, A. J., A. Voronovich, B. L. Weber, B. Standkov, M. Klein, R. J. Hill, and J. W. Bao, "Geosynchronous microwave (GEM) sounder/imager observation system simulation," *Proceedingss of IGARSS 2003*, 1209–1211, Jul. 2003.
5. Bizzarri, B., A. J. Gasiewski, and D. Staelin, "Observing rain by millimetre — Submillimetre wave sounding from geostationary orbit," *Series on Advances in Global Change Research*, Ch. 50, 675–692, Springer, New York, 2007.
6. "Statement of guidance regarding how well satellite capabilities meet WMO user requirements in several application areas," WMO Report, WMO TD No. 992 (Sat-22), Geneva, Switzerland, 2000.
7. Eyre, J. R., "The information content of data from satellite sounding systems: A simulation study," *Quarterly Journal of the Royal Meteorological Society,* Vol. 116, 401–434, Dec. 2006.
8. Purser, R. J. and H.-L. Huang, "Estimating effective data density in a satellite retrieval or an objective analysis," *Journal of Applied Meteorology,* Vol. 32, 1092–1107, Jun. 1993.
9. Huang, H.-L. and R. J. Purser, "Objective measures of the information density of satellite data," *Meteorology and Atmospheric Physics*, Vol. 60, 105–117, Mar. 1996.
10. Rodgers, C. D., "Information content and optimization of high spectral resolution measurements," *Proceedings of SPIE*, Vol. 2830, 136–147, Oct. 1996.
11. Klein, M. and A. J. Gasiewski, "The sensitivity of millimeter and sub-millimeter frequencies to atmospheric temperature and water vapor variations," *Journal of Geophysical Research,* Vol. 13, 17481–17511, Jul. 2000.
12. Lipton, A. E., "Satellite sounding channel optimization in the microwave spectrum," *IEEE Transactions on Geoscience and Remote Sensing*, Vol. 41, 761–781, Apr. 2003.
13. Prigent, C., J. R. Pardo, and W. B. Rossow, "Comparisons of the millimeter and submillimeter bands for atmospheric temperature and water vapor soundings for clear and cloudy skies," *Journal of Applied Meteorology and Climatology*, Vol. 45, 1622–1633, Dec. 2006.
14. Bizzarri, B., "Geostationary observatory for microwave atmospheric sounding," *Report to the Second Call for Proposals for ESA Earth Explorer Opportunity Missions*, 2002.
15. Borbas, E. E., S. W. Seemann, H.-L. Huang, J. Li, and W. P. Menzel, "Global profile training database for satellite regression retrievals with estimates of skin temperature and emissivity," *Proceedings of the XIV. International ATOVS Study Conference,* 763–770, May 2005.
16. Peckham, G. E., "Multiresolution analysis, entropic information and the performance of atmospheric sounding radiometers," *Quarterly Journal of the Royal Meteorological Society*, Vol. 126, 2933–2949, Apr. 2000.